

Surface-Based Atlases of Cerebellar Cortex in the Human, Macaque, and Mouse

DAVID C. VAN ESSEN

Department of Anatomy and Neurobiology, Washington University School of Medicine, St. Louis, Missouri 63110, USA

ABSTRACT: This study describes surface reconstructions and associated flat maps that represent the highly convoluted shape of cerebellar cortex in three species: human, macaque, and mouse. The reconstructions were based on high-resolution structural MRI data obtained from other laboratories. The surface areas determined for the fiducial reconstructions are about 600 cm² for the human, 60 cm² for the macaque, and 0.8 cm² for the mouse. As expected from the ribbon-like pattern of cerebellar folding, the cerebellar flat maps are elongated along the axis parallel to the midline. However, the degree of elongation varies markedly across species. The macaque flat map is many times longer than its mean width, whereas the mouse flat map is only slightly elongated and the human map is intermediate in its aspect ratio. These cerebellar atlases, along with associated software for visualization and for mapping experimental data onto the atlas, are freely available to the neuroscience community (see <http://brain-map.wustl.edu>).

KEYWORDS: cerebellar cortex; atlas; humans; macaques; mice

INTRODUCTION

The most striking gross morphologic feature of the cerebellum is its highly convoluted cortical mantle. The convolutions allow a large cortical surface area to be contained within a compact cerebellar volume, but they present a major obstacle to experimentalists interested in analyzing diverse aspects of cerebellar structure and function.

A valuable approach to dealing with a convoluted cortex is to generate surface reconstructions that capture the shape of the convolutions and can be inflated and flattened to facilitate visualization of buried cortex. This strategy has been applied very successfully to the cerebral cortex, especially in humans and macaques.¹⁻³ Extending the same strategy to the cerebellar cortex has proven more challenging, because it is much thinner (about one third as thick as cerebral cortex) and its convolutions are more complex. In many species, including human and macaques, the convolutions span several scales, from large cerebellar lobules to medium-sized lamellae, to

Address for correspondence: Department of Anatomy and Neurobiology, Washington University School of Medicine, 660 S. Euclid Ave., Box 8108, St. Louis, MO 63110. Voice: 314-326-7043; fax: 314-747-3436.
vanessen@v1.wustl.edu

Ann. N.Y. Acad. Sci. 978: 468–479 (2002). © 2002 New York Academy of Sciences.

fine-grained folia. To reconstruct the surface, it is necessary to obtain structural data in which the cerebellar folds are accurately visualized and are in register across neighboring slices.

Presented here are the first surface reconstructions that represent the overall pattern of convolutions in human, macaque, and mouse cerebellum. These reconstructions, based on high-resolution structural magnetic resonance imaging (MRI) data, faithfully represent the cerebellar lobules and lamellae, and they capture many but not all of the finer-grained folia. They differ from previously reported cerebellar surface reconstructions that represented the shape of the external cerebellar hull but not the complexity of its convolutions.^{4,5} In this chapter, reconstructions are used for two main purposes: to examine the intrinsic geometry of the cerebellar sheet and to illustrate the potential of surface-based cerebellar atlases for visualizing many types of experimental information.

A distinctive aspect of cerebellar surface geometry is that the folds tend to run parallel to one another, as in an accordion or a piece of ribbon candy. One might therefore expect that the unfolded cerebellar ribbon would be highly elongated. Indeed, the cerebellar flat maps that Sultan and Braitenberg⁶ generated from a variety of species using an indirect, semiquantitative mapping procedure were all highly elongated. On the other hand, the geometry is complicated by extensive branching and fusion of sulci in the cerebellar hemispheres. As shown here, computationally generated cerebellar flat maps vary greatly in shape: the macaque map is highly elongated, but the mouse map is not, and the human map is intermediate.

Surface-based atlases are useful for viewing many types of spatially localized experimental data that are brought from individuals onto a common atlas framework. This is well established for the cerebral cortex, where current atlases include, for example, a diversity of areal partitioning schemes, information about anatomic connectivity, and a variety of neuroimaging data.^{3,7,8} The cerebellar surface reconstructions illustrated here, along with associated surface visualization and analysis software, are freely available, and they provide an attractive substrate for representing a large and rapidly growing body of information about the cerebellar cortex.

METHODS

Surface reconstructions were based on high resolution structural MRI data sets (T1-weighted) obtained for mouse, macaque, and human. The mouse data set (case map015, provided by A. Toga and R. Jacobs) was scanned at $56 \mu\text{m}^3$ voxel size; the macaque data set (case F99UA1, provided by N. Logothetis) was scanned at 0.5 mm^3 voxel size. The human data set (case colin_avg20, provided by A. Toga) was from an individual subject scanned repeatedly at 1 mm^3 voxel size; the individual scans were registered to a common stereotaxic space, averaged, and resampled to 0.5 mm^3 voxel size. This is the same case described in a study by Holmes *et al.*⁹ and in the cerebellar atlas of Schmahmann *et al.*⁵ In the human case the contrast between gray and white matter was significantly lower in ventral than in dorsal portions of the cerebellum, perhaps because of regional differences in the accuracy of the registration algorithm.

For each species, the whole brain MRI volume was cropped to include just the cerebellum. It was then resampled so that the cerebellar cortex was about two or three voxels thick on average. The resampled volumes had voxel dimensions of 84 m^3 for the mouse, 0.25 mm^3 for macaque, and 0.5 mm^3 for human. A modification of the SureFit segmentation method, originally developed for cerebral cortex,¹ was applied to the structural MRI volumes to generate a binary volume (segmentation) whose boundary represents the shape of the cerebellar cortex, including its convolutions. The general SureFit strategy involves generating probabilistic maps related to characteristics of gray matter, white matter, and cerebrospinal fluid (CSF) that are discernible in the image data. Most of cerebellar white matter (except for the central core) is very thin and cannot be robustly identified on the basis of intensity cues alone. A more reliable cue is that thin slabs of white matter are adjoined on either side by slabs of gray matter. Consequently, the image intensity gradient in such regions should be pointed towards the white matter on two opposing sides and should have an appropriate intermediate magnitude (based on the average intensity difference between gray and white matter and the average cortical thickness). An algorithm sensitive to such patterns at any arbitrary three-dimensional orientation was used to generate a probabilistic map of cerebellar white matter. An analogous process was used to generate a probabilistic map for the outer cortical boundary (the pial surface). This was based on the cue that in regions of CSF sandwiched between opposing banks of gray matter, the intensity gradient should be pointed away from the CSF and should have an appropriate magnitude (based on the average intensity difference between gray matter and CSF and on cortical thickness). The maps of thin white matter and of the outer boundary maps were combined to form a probabilistic map of position along the radial axis of cortical gray matter. The radial position map was then thresholded to yield an initial segmentation whose boundary on average ran approximately midway through the cortical gray matter. To the extent that this is achieved, each unit area on the associated surface reconstruction represents a comparable amount of cortex, irrespective of whether it is at the tip or the base of a lobule.¹⁰ The initial segmentations generated with this method contained numerous topological errors, which generally reflect ambiguities associated with low contrast and noise in the original image data. Extensive error correction using an interactive editing tool in SureFit was used to achieve a topologically correct segmentation for each species. For each corrected cerebellar segmentation, a surface reconstruction whose nodes lie on the boundary of the segmented volume was generated in SureFit. This slightly blocky “raw” surface was smoothed to generate a fiducial surface that constitutes the best available estimate of cortical shape.

Cortical flattening was achieved using Caret surface visualization and analysis software.^{1,11} For the mouse, cerebellar flattening involved straightforward application of the automated Caret multiresolution method for flattening and distortion reduction.¹² For the macaque and human, flattening was applied piecemeal to restricted subregions of the cerebellar surface. This was necessary because of the inherent difficulty in flattening a highly irregular cerebellar surface that has a far higher degree of intrinsic (Gaussian) curvature than does the cerebral cortex (akin to the fingers on a rubber glove rather than the folds of a crumpled sheet). Once the individual subregions were satisfactorily flattened, they were combined into a composite whole, and the map was locally smoothed in the vicinity of the sutures.

RESULTS

The results are presented in a similar format for each species, including images of the structural MRI data and the segmented cerebellar volume plus surface reconstructions in multiple configurations and viewing perspectives. The mouse cerebellum is illustrated first, as its relatively simple geometry provides a useful baseline for comparisons with the macaque and human.

Mouse Cerebellum

In the structural MRI volume used for the mouse atlas, the cerebellar gray and white matter can readily be discriminated, as shown in a sagittal slice (FIG. 1, top left). The adjacent panel (FIG. 1, top center) shows the segmented cerebellar cortex, whose boundary runs consistently through the cortical gray matter. Comparison with the Nissl-stained cerebellar sections from a mouse brain atlas¹³ indicates that the full pattern of cerebellar folds is visible in the structural MRI images and is preserved in the segmented volume. The cerebellar lobules, identified with the aid of this atlas, are labeled on the segmented slice.

The remaining panels of FIGURE 1 show different configurations and viewing perspectives of the mouse cerebellar surface reconstruction. Fiducial, inflated, and spherical configurations are shown from posterior and lateral perspectives in the left and upper right parts of the figure, respectively. The fiducial surface reveals the shape of the intact cortex. In the inflated surface the folds are largely smoothed out, but the overall cerebellar shape is preserved. The spherical map provides a useful substrate for surface-based coordinates and surface-based registration (see Discussion). The flat map, which shows the entire cerebellar surface in a single view, is displayed in the lower right part of FIGURE 1. The location of the cuts made to reduce distortions on the flat map are best seen on the spherical and inflated maps. All of the surfaces are shaded to show surface folding (computed on the fiducial configuration), with light creases signifying outward folds along lobule crests and dark creases signifying inward (sulcal) folds.

The total cerebellar surface area for the fiducial configuration is 80 mm², which is about half the combined cortical surface area of the left and right cerebral hemispheres reconstructed from the same mouse atlas (174 mm²). Sultan and Braitenberg⁶ reported a much larger cerebellar surface area (190 mm² average for three mice), but it is difficult to evaluate whether systematic biases affected their indirect measurement strategy.

Overall, the cerebellar flat map is about as wide as it is long, making its shape quite different from the approximately threefold elongated map for the schematically unfolded mouse cerebellum illustrated by Sultan and Braitenberg.⁶ The vermis, which occupies 43% of the fiducial surface area, forms an elongated strip along the vertical axis. The cerebellar hemispheres, on the left and right sides of the map, predominantly involve expansions of lobules VI–VIII and occupy 51% of the fiducial surface. The adjoining paraflocculus and flocculus (6% of the fiducial surface) are extensions from the copula (lobule VII) and paramedian lobule (lobule VIII).

As with maps of cerebral cortex, there are substantial distortions in the representation of cortical surface area on the cerebellar flat map and spherical map (particu-

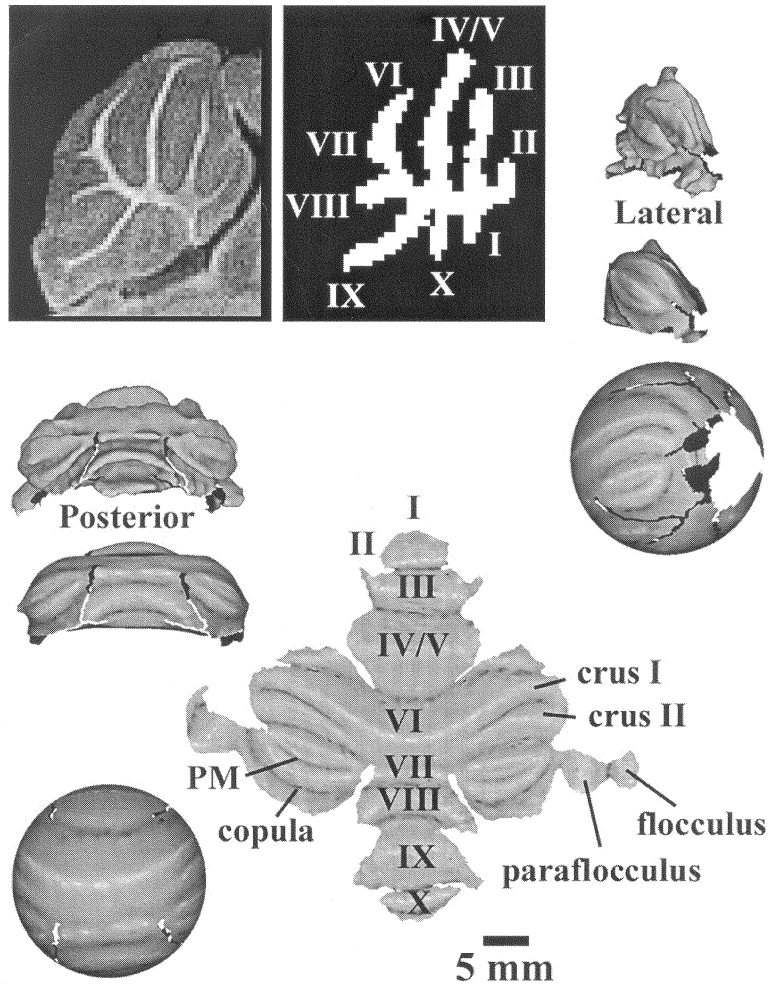


FIGURE 1. A surface-based atlas of mouse cerebellar cortex. *Upper left* and *upper center* panels show the structural MRI and segmentation (with lobules identified) from a sagittal section through the vermis. The remaining panels show cerebellar surface reconstructions, with posterior views of the fiducial, inflated, and spherical surface shown on the *left*, lateral views of the same three configurations on the *right*, and a flat map in the *lower center*.

larly on the spherical map because it is geometrically more constrained). Although it is important to know that these distortions exist, they are not a major impediment to quantitative analyses, because the surface area of any region of interest on a flat map or spherical map can readily be computed for the corresponding region on the fiducial surface (as illustrated in the preceding paragraph). Having a topologically correct spherical surface allows location to be specified by spherical coordinates of

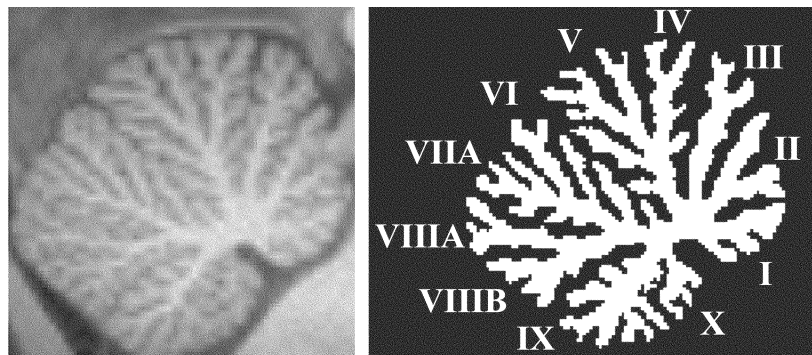


FIGURE 2. Sagittal sections through cerebellar vermis of the macaque monkey. (*Left*) Structural MRI; (*right*) cortical segmentation.

latitude and longitude,^{14,15} in which nearby points on the cerebellar surface always have similar coordinates.

Macaque Cerebellum

The vastly greater complexity of cerebellar folding in the macaque than in the mouse is obvious in a midline sagittal view of the structural MRI (FIG. 2, left). I assessed the fidelity of the structural MRI by making comparisons to sagittal sections of adult macaque cerebellum shown in tracings by Larsell and Jansen¹⁶ (their Figs. 176–177). A comparable number of distinct folia (~90–100) can be discerned in sagittal slices from both data sets. This implies that the structural MRI data used here reveals nearly all of the cerebellar convolutions, at least along the midline. In the segmented volume (FIG. 2, right), all of the lobules and major lamellae are successfully represented, as are a majority of the individual folia. However, about a third of the folia are not explicitly captured in the segmentation, owing to their small size combined with image noise and low contrast. In more lateral regions (not shown in FIGURE 1), the detailed structure of the flocculus was difficult to discern, and it was not included in the segmentation.

FIGURE 3 shows the macaque cerebellar surface reconstruction, with fiducial, inflated, and spherical configurations displayed from posterior views on the left and lateral views on the right. The total surface area of the fiducial configuration is 61 cm², which is 25% of total cerebral cortex for the left and right hemispheres (248 cm², respectively) and is close to the value of 81 cm² for the macaque reported by Sultan and Braitenberg.⁵ It is almost 80-fold greater than the surface area of the mouse atlas cerebellum.

Compared to the mouse, not only are the convolutions of macaque cerebellar cortex deeper and more numerous, but also the overall pattern in the hemispheric regions is more complex. About 65% of the fiducial surface area is associated with the two hemispheres versus 33% for the vermis and 2.4% for the portion of the paraflocculus included in the segmentation. The hemispheric portions of lobules VII and VIII have a disproportionately large surface area, and they form a ribbon that curls

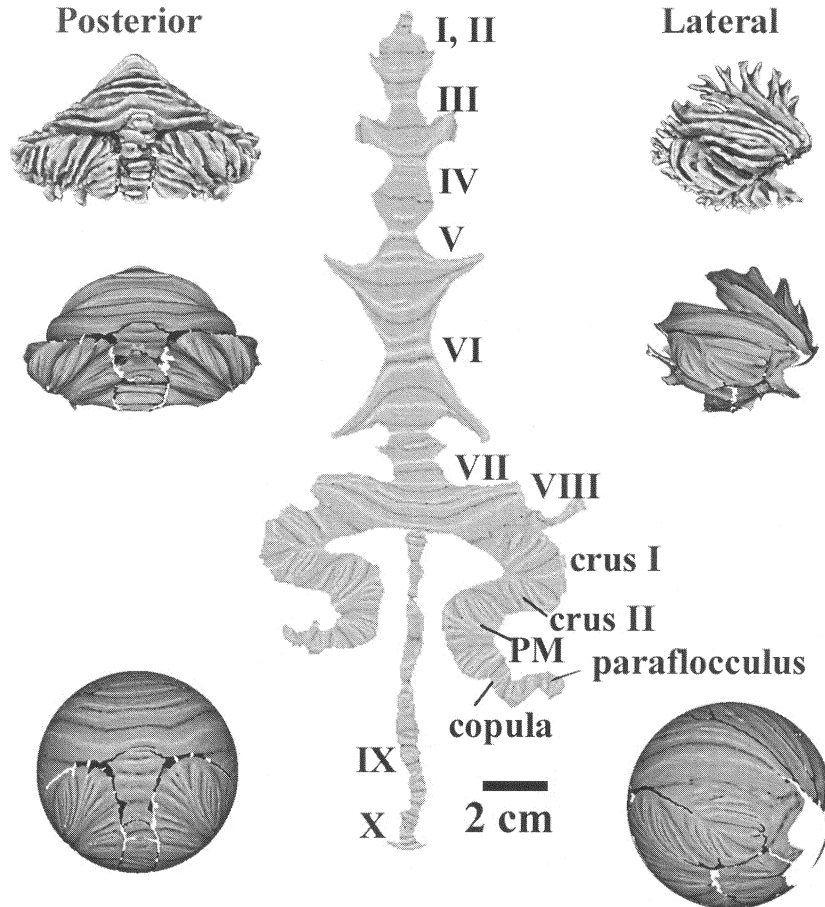


FIGURE 3. Surface representations of the macaque cerebellar cortex. (*Left*) Posterior views of the fiducial, inflated, and spherical surface. (*Right*) Lateral views of the same three configurations. (*Center*) Cerebellar flat map.

from lateral back towards the midline, ventral to the shelf formed by lobule VI. Along the boundary between the posterior vermis and lobule VIII, the cortex is not physically continuous. Instead, there are natural terminations, evident in stained sections from a macaque atlas,¹⁷ although they are not directly discernible in the structural MRI data. The cuts used to reduce distortions in the flat map were made along the estimated trajectory of these natural cortical boundaries. To avoid severe distortions, it was necessary to make many additional cuts that interrupted genuinely contiguous cortical regions, as can be seen in the inflated and spherical maps.

Because the macaque vermis is relatively narrow (4–6 mm) but has deep and complex folds (cf. FIG. 2), it forms a highly elongated strip that runs vertically on the flat map. In the upper part of the map, the hemispheric portions of lobules I–VI appear as stubby flanges attached to the vermis, reflecting the fact that lobules I–VI become progressively shallower and simpler in more lateral portions of the fiducial surface.

In contrast, the hemispheric portions of lobules VII and VIII form prominent “legs” whose elongated but bowed shape largely reflects the ribbon-like configuration of this region in the fiducial surface.

Human Cerebellum

In a sagittal view, the structural MRI of the human cerebellar vermis (FIG. 4, left) shows about the same apparent degree of complexity as shown in the corresponding slice through the macaque cerebellum (cf. FIG. 2) in terms of the number of lobules and lamellae. However, the overall image quality is somewhat lower for the human MRI data set compared to the macaque, particularly in the ventral cerebellum (see Methods). In reality, the human vermis is substantially more convoluted than that in the macaque, as sagittal section tracings^{18,19} reveal about twice as many small folia visible on each of the lobules as in the macaque. Because of the lower image quality, the segmented human cerebellum (FIG. 4, right) certainly missed most of these smaller folia, but it successfully represents all lobules, most or all lamellae, and many individual folia. The lobules were identified using published atlases.^{5,18}

FIGURE 5 shows the human cerebellar surface reconstruction, with fiducial, inflated, and spherical configurations shown from posterior views on the left and lateral views on the right. The total surface area of the fiducial configuration is 540 cm². This is about ninefold greater than the macaque cerebellum and is 28% of the total cerebral cortex for the left and right hemispheres combined (1,900 cm²). This is certainly a substantial underestimate because, as just noted, many cerebellar folia were missed in the segmentation. The larger estimate of 1,128 cm² for human cerebellum reported by Sultan and Braitenberg⁶ is likely to be more accurate. Not surprisingly, the spherical map is severely compressed in some regions, expanded in others, and anisotropically stretched in others. However, the fact that it preserves the topology

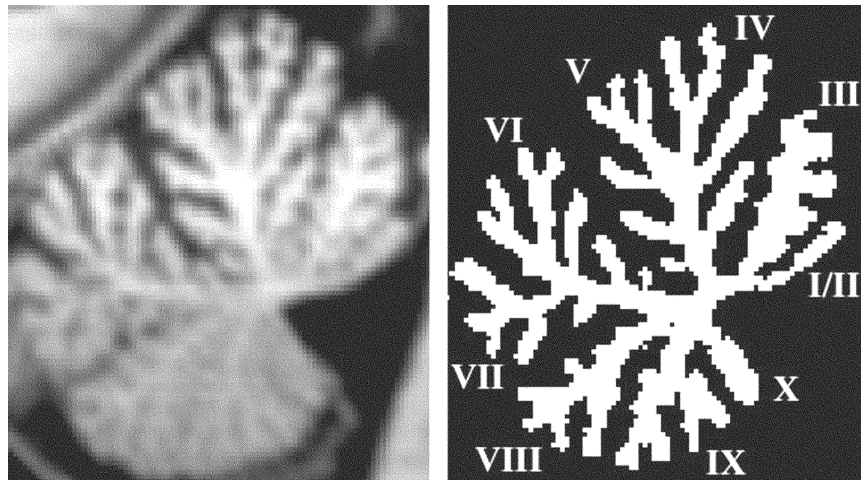


FIGURE 4. Sagittal sections through the human cerebellar vermis. (*Left*) Structural MRI; (*right*) cortical segmentation.

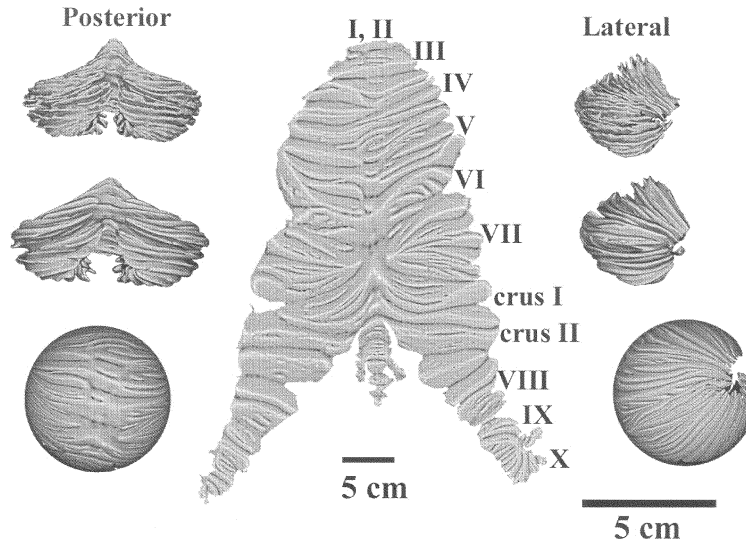


FIGURE 5. Surface representations of the human cerebellar cortex. (*Left*) Posterior views of the fiducial, inflated, and spherical surface. (*Right*) Lateral views of the same three configurations. (*Center*) Cerebellar flat map.

of the cortical sheet gives it utility as a substrate for surface-based coordinates and surface-based registration.

In comparing human and macaque cerebellum, the most striking difference is the greater elaboration of hemispheric cortex in all lobules, with an estimated 88% of human cerebellar cortex identified as hemispheric in the fiducial configuration. Also, the representation of hemispheric portions of all lobules is more balanced than in the macaque. In the more anterior lobules (I–III), this arises because the hemispheric regions are relatively wide and retain about the same number and depth of lamellae over most of their width. For the more posterior lobules, the expansion reflects convolutions that are markedly deeper and more numerous. These characteristics result in a human cerebellar flat map that is relatively wide throughout and is not nearly as elongated as in the macaque or as in the schematic unfolding shown by Sultan and Braitenberg.⁶

DISCUSSION

Cerebellar Geometry and Development

The distinctive surface geometry of cerebellar cortex reflects several key aspects of cerebellar morphogenesis. The cerebellum receives its full complement of Purkinje cells very early in development, before extensive convolutions have formed. The immature Purkinje cells are initially stacked many cells deep, especially in the hemispheric regions of the cerebellar plate.¹⁹ The vastly more numerous granule cells

proliferate extensively as they migrate tangentially along the external granule cell layer. The granule cells extend parallel fiber axons before diving down to the granule cell layer, thereby establishing an axis that is correlated with the pattern of folding and anisotropic growth in surface area.²⁰ An attractive hypothesis is that mechanical tension along parallel fibers is responsible for both the anisotropic growth (preferential expansion along the axis orthogonal to parallel fibers) and the axis of folding parallel to that of the parallel fibers.²¹

Cerebral cortex has a very different surface geometry that reflects its very different pattern of morphogenesis. For cerebral cortex, a thin, smooth, balloon-like cortical sheet forms early in development as a result of cell proliferation in the ventricular zone and migration along the radial axis. The increases in cerebral cortical surface area arise mainly from cell growth rather than differential migration. The formation of cortical folds is probably caused by mechanical tension along long-distance corticocortical connections as they are established.²¹ Because the convolutions arise, in effect, from crumpling of a quasispherical cortical balloon, the distortions are relatively modest during the reverse process of smoothing out the convoluted adult cerebral cortex.

Surface-Based Cerebellar Atlases

Brain atlases provide natural gateways for navigating and visualizing an immense range of neuroscientific data.^{8,11,22} For cortical structures, surface-based atlases are especially valuable, because they provide flexible visualization options, plus they can be used for registering data across individuals and across species, and as a substrate for surface-based coordinates that respect the topology of the cortical sheet.^{3,7,8,15}

The maps of cerebellar cortex presented here are intended for general use as surface-based atlases. The atlas data sets for all three species are freely available, along with associated surface visualization software.²⁶ The structural volume data are also available and can be viewed with freely available volume visualization software.^{23,24} Data that are currently available on the atlas (not shown here because of space constraints) include representations of cerebellar geography (individual lobules identified and painted different colors) plus exemplar functional MRI data on the human cerebellar maps.

A variety of currently available tools for data mapping should allow the amount of experimental data mapped to cerebellar atlases to increase rapidly. These include options for registering data from individual sections or from surface reconstructions of part or all of the cortex. An additional option is to map individual neuroimaging activation foci or entire fMRI volumes that are represented in stereotaxic space.

Interspecies Comparisons

The major cerebellar lobules can consistently be identified in mouse, macaque, and human, and they emerge from a common developmental pattern.^{16,18} Presumably there are important functional correspondences between lobules of the same name, but the degree of correspondence is not well established in detail. Making such comparisons entails dealing with major species differences in folding patterns and in the relative sizes of different lobules and their internal subdivisions. There is

also the prospect that the basic topology of cerebellar organization may differ markedly across species. The availability of spherical maps for the cerebellum should facilitate interspecies comparisons because it allows mappings that preserve the topology of the cortical sheet, analogous to those that have proven useful for interspecies comparisons of cerebral cortex.^{25,26}

ACKNOWLEDGMENTS

This work was supported by a Human Brain Project/Neuroinformatics research grant funded jointly by the National Institute of Mental Health, National Science Foundation, National Cancer Institute, National Library of Medicine, and the National Aeronautics and Space Administration (R01 MH60974-06). I thank J. Harwell and D. Hanlon for software development and T. Thach for advice.

REFERENCES

1. VAN ESSEN, D.C., J. DICKSON J. HARWELL, *et al.* 2001. An integrated software system for surface-based analyses of cerebral cortex. *J. Am. Med. Inform. Assoc.* **8**: 443–459.
2. DALE, A.M., B. FISCHL & M.I. SERENO. 1999. Cortical surface-based analysis. I. Segmentation and surface reconstruction. *NeuroImage* **9**: 179–194.
3. VAN ESSEN, D.C. 2002. Organization of visual areas in macaque and human cerebral cortex. *In The Visual Neurosciences*. L. Chalupa & J.S. Werner. MIT Press. In press.
4. HURDAL, M.K., P.L. BOWERS, K. STEPHENSON, *et al.* 1999. Quasi-conformally flat mapping the human cerebellum, *In Medical Image Computing and Computer-Assisted Intervention-MICCAI'99*, Vol. 1679. Lecture Notes in Computer Science. C. Taylor & A. Colcheste, Eds. :279–286. Springer. Berlin.
5. SCHMAHMANN, J.D., J. DOYON, D. McDONALD, *et al.* 1999. Three-dimensional MRI atlas of the human cerebellum in proportional stereotaxic space. *NeuroImage* **10**: 233–260.
6. SULTAN, F. & V. BRAITENBERG. 1993. Shapes and sizes of different mammalian cerebella. A study in quantitative comparative neuroanatomy. *J. Hirnforsch.* **34**: 79–92.
7. VAN ESSEN, D.C. & H.A. DRURY. 1997. Structural and functional analyses of human cerebral cortex using a surface-based atlas. *J. Neurosci.* **17**: 7079–7102.
8. VAN ESSEN, D.C. 2002. Windows on the brain: the emerging role of atlases and databases in neuroscience. *Curr. Opin. Neurobiol.* **12**: 574–579.
9. HOLMES, C.J., R. HOGE, I. COLLINS, *et al.* 1998. Enhancement of MR images using registration for signal averaging. *J. Comput. Assist. Tomogr.* **22**: 324–333.
10. VAN ESSEN, D.C. & J.H.R. MAUNSELL. 1980. Two-dimensional maps of the cerebral cortex. *J. Comp. Neurol.* **191**: 255–281.
11. VAN ESSEN, D.C., H.A. DRURY, J. HARWELL & D. HANLON. 2002. CARET User's Guide and Tutorial. Part II. Surface Manipulation, Flattening, and Surface-Based Registration. Accessible at http://brainmap.wustl.edu/caret/pdf/caret_user_guide_part2.pdf
12. DRURY, H.A., D.C. VAN ESSEN, C.H. ANDERSON, *et al.* 1996. Computerized mappings of the cerebral cortex. A multiresolution flattening method and a surface-based coordinate system. *J. Cogn. Neurosci.* **8**: 1–28.
13. PAXINOS, G. & K.B.J. FRANKLIN. 2000. *The Mouse Brain in Stereotaxic Coordinates*, 2nd ed. Academic Press. New York.
14. FISCHL, B., M.I. SERENO & A.M. DALE. 1999. Cortical surface-based analysis. I. Inflation, flattening, and a surface-based coordinate system. *NeuroImage* **9**: 195–207.
15. FISCHL, B., M.I. SERENO, R.B. TOOTELL & A.M. DALE. 1999. High-resolution intersubject averaging and a coordinate system for the cortical surface. *Hum. Brain Mapping* **8**: 272–284.

16. LARSELL, O. & J. JANSEN. 1970. *The Comparative Anatomy and Histology of the Cerebellum from Monotremes through Apes*. University of Minnesota Press. Minneapolis.
17. PAXINOS, G., X.-F. HUANG & A.W. TOGA. 2000. *The Rhesus Monkey Brain in Stereotaxic Coordinates*. Academic Press. New York.
18. LARSELL, O. & J. JANSEN. 1972. *The Comparative Anatomy and Histology of the Cerebellum. The Human Cerebellum, Cerebellar Connections, and Cerebellar Cortex*. University of Minnesota Press. Minneapolis.
19. RAKIC, P. & R.L. SIDMAN. 1970. Histogenesis of cortical layers in human cerebellum, particularly the lamina dissecans. *J. Comp. Neurol.* **139**: 473–500.
20. SIDMAN, R.L. & P. RAKIC. 1973. Neuronal migration, with special reference to developing human brain: a review. *Brain Res.* **62**: 1–35.
21. VAN ESSEN, D.C. 1997. A tension-based theory of morphogenesis and compact wiring in the central nervous system. *Nature* **385**: 313–318.
22. TOGA, A.W. & P.M. THOMPSON. 2002. New approaches in brain morphometry. *Am. J. Geriatr. Psychiatry* **10**: 13–23.
23. VAN ESSEN, D.C., H.A. DRURY, D. HANLON & J. HARWELL. 2002. User's Guide to SureFit Cortical Segmentation and Surface Reconstruction. Accessible at <http://brainmap.wustl.edu/SureFit/SureFitUsersGuide.pdf>
24. COX, R.W. AFNI: Introduction, Concepts, and Principles. URL: <http://afni.nimh.nih.gov/afni/edu>
25. VAN ESSEN, D.C., H.A. DRURY, S. JOSHI & M.I. MILLER. 1998. Functional and structural mapping of human cerebral cortex: solutions are in the surfaces. *Proc. Natl. Acad. Sci. USA* **95**: 788–795.
26. VAN ESSEN, D.C., H.A. DRURY, J. HARWELL & D. HANLON. 2002. CARET User's Guide and Tutorial. Part I. Surface-Based Atlases of Cerebral and Cerebellar Cortex in Human, Macaque, and Mouse. Accessible at http://brainmap.wustl.edu/caret/pdf/caret_user_guide_part1.pdf